H-Band SPDT Waveguide Switch Based on Glide-Symmetric Electromagnetic Bandgap Structures

H-Band SPDT Waveguide Switch Based on Glide-Symmetric Electromagnetic Bandgap Structures

Jorge Martín-Villar*, Martin Petek*, Jorge Tobon Vasquez**, Zhongxia Simon He†‖, Francesca Vipiana*
*Dept. of Electronics and Telecommunications, Politecnico di Torino, Torino, Italy, jorge_martin@polito.it
†Sinowave, Götheborg, Sweden, simon@sinowave.se
‖Aerospace and Informatics Domain, Beijing Institute of Technology, Zhuhai, China
**Wavision srl, Torino, Italy, jorge.tobonvasquez@polito.it

***Abstract*—This work presents the design and analysis of a single-pole double-throw (SPDT) waveguide switch implemented using multilayer waveguide (MLW) technology. The proposed fully metallic air-filled structure operates in the H-band (220–330 GHz) and employs a glide-symmetric unit cell acting as an electromagnetic bandgap (EBG) material to suppress leakage and improve manufacturing tolerance. The SPDT enables signal routing between two output branches through a rotating metallic part. The design achieves insertion losses below 2 dB and return losses better than 10 dB across most of the H-band.**

***Index Terms*—glide symmetry, H-band, multilayer waveguide, SPDT.**

I. Introduction

The sub-THz band ($100-300$ GHz) is suitable for extremely high data-rate links which are critical for supporting emerging applications. Representative use cases include high-bitrate datalinks for 6G systems, last-mile connectivity in scenarios where optical fiber cannot be deployed, point-to-point wireless backhaul, and ultra-fast intra-rack communications in data centers [1], [2].

Designing and manufacturing components that operate at these frequencies is both challenging and expensive, as they require high precision and strict tolerances. For waveguides, the most straightforward approach is to employ hollow metallic structures, as they offer low losses and are well suited for high-power applications. Nevertheless, the need for highly accurate dimensional control makes their fabrication process complex and costly [3]. On the other hand, planar technology provides cost-effective fabrication processes at high frequencies and is compact, even allowing easy integration into printed circuit boards. However, the presence of dielectric materials makes these structures lossy and, therefore, not ideal for the H-band (220–330 GHz). Gap waveguides [4], [5] consists of two metallic plates, each including a waveguide channel and a periodic structure. When the top and bottom plates are assembled together, separated by a small gap, the periodic structure prevents leakage. This periodic structure is usually done with pins and their fabrication becomes increasingly challenging at high frequencies because the size of the pins becomes smaller.

An alternative in implementing waveguides is stacking several etched metallic layers. This technology is called MLW and it allows to build fully metallic structures, having the advantages of the hollow waveguides in terms of low losses and power handling. Additionally, since they consist of stacked metallic sheets, the manufacturing process becomes cost effective and suitable for mass production. However, this introduces possible gaps between layers as a result of manufacturing intolerances [6]. This can be solved placing a periodic structure to act as an EBG material to prevent leakage, e.g. with glide-symmetric holes [7]. Glide symmetry refers to a periodic structure in which consecutive layers are mirrored and shifted by half a period, providing a wider bandwidth [8].

However, the development of components operating at H-band with MLW technology has not fully exploited its potential. In particular, single-pole double-throw (SPDT) switches are typically implemented using integrated circuits, which introduce undesired losses [9].

Hence, in this paper, we design and analyze a SPDT switch realized with MLW technology. The proposed SPDT enables wave transmission switching between two output branches, with good reflection and transmission performance in almost the whole H-band.

II. Design

The design of the switch in the MLW configuration is a two-step procedure. First, the EBG structure is designed such that the operating band is centered within the stopband. This ensures confinement of the electric field within the groove.

Secondly, the SPDT structure is designed by positioning the waveguide channels and the rotating part. The EBG structure is then placed close to the boundaries of the groove.

A. *Multilayer unit cell analysis*

In this subsection, an analysis of the unit cell with multiple layers is performed. The structure is shown in Fig. 1. The design is composed of square holes that are mirrored over the xy-plane at the center of each gap and shifted by half a period, constructing a locally glide symmetric structure. The term 'locally glide symmetric' here means that two adjacent layers are glide-symmetric, although the total structure is not glide-symmetric . The dimensions of the structure are shown in Table I.

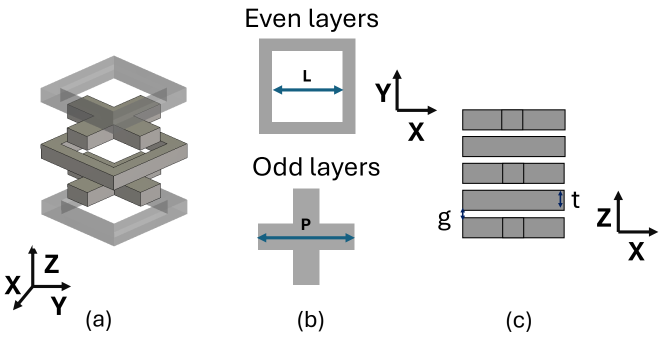

Fig. 1. (a) 3D Unit cell view. (b) Unit cell top-down view. (c) Unit cell side view.

TABLE I
GEOMETRICAL DIMENSIONS

Parameter	Dimension (μm)	Description
Unit cell		
L	480	Square hole width
P	980	Unit cell period
t	100	plate thickness
g	10	Gap between layers
Waveguide		
W1	24000	Plate width
W2	860	Waveguide port width
H	432	Port height
L1	18616	Right branch
L2	18616	Left branch
R	560	Rotating part radius

The dispersion diagram of the proposed unit cell is presented in Fig 2. The dispersion diagram is obtained through simulations performed using CST Eigensolver (ES). The stopband of the structure extends from 208 to 373 GHz, thus fully covering the H-band.

B. H-band switch

This subsection presents the design and analysis of the MLW SPDT intended for the H-band. The main purpose of the SPDT is to switch between branches, allowing transmission only through one branch or the other. The leakage that can be produced between layers is suppressed by an EBG structure. In our simulations, the gap between these layers is considered as shown in Table I, following the values established in previous works [6].

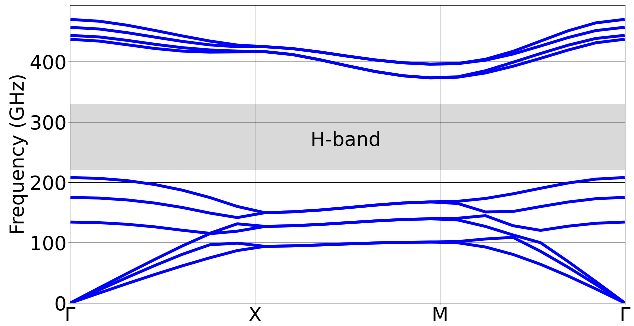

Fig. 2. Dispersion Diagram. The results of the CST ES shows that the unit cell covers the entire H-band)

The complete design of the structure is illustrated in Fig. 3, showing a three-dimensional view of the entire assembly. The device consists of three distinct waveguide channels and a central rotating element. The design includes three different ports: one input (Port 1) and two outputs (Ports 2 and 3). Vertical transitions are placed at all ports to match the input and output signals from vertical to horizontal configuration. The switching part is located in the central region of the structure. The material chosen for the simulations is silver, since it has low losses and is one of the materials that can be used for coating in the manufacturing process. Figure 4 provides a detailed 3D view of the rotating part, where the groove introduces a 90° bend. In order to understand how the structure rotates, Fig.,5 is helpful for clarification. There, the parameter ξ_1 represents a local vector that rotates with the structure. ϕ is the angle between ξ_1 and the y-axis, and it is defined as the rotational angle of the rotating part. Thus the structure rotates in anti-clockwise direction 0° and 90° to connect the bottom waveguide channel to either right or left branch.

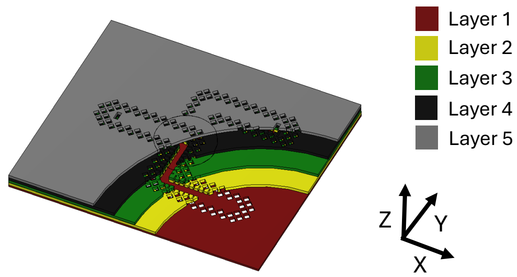

Fig. 3. Designed structure containing two different branches that can be chosen using the switch. The structure is shown partially cut to make the stack-up clearer

The S-parameter analysis is performed by first setting the structure at an angle of 0°, which corresponds to selecting the left branch, producing $S_{11}(\varphi = 0°)$ and S_{21}. Subsequently, the angle is set at 90° to select the right branch, from which

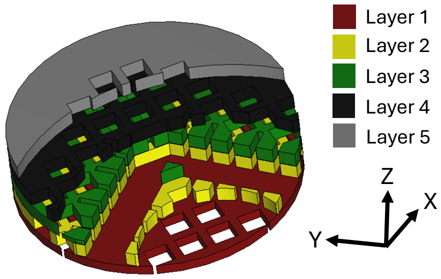

Fig. 4. Rotating part of the switch. This component rotates to select which branch is active.

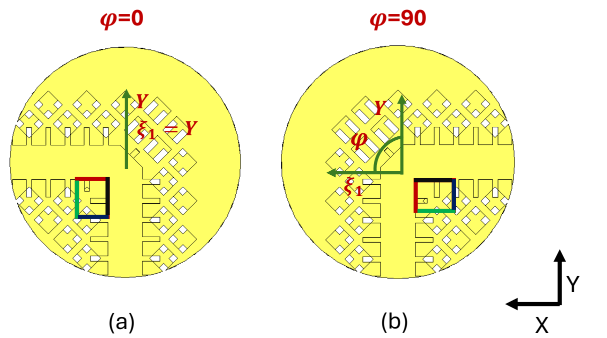

Fig. 7. Rotational asymmetry of the structure. This affects the S-parameter behavior.

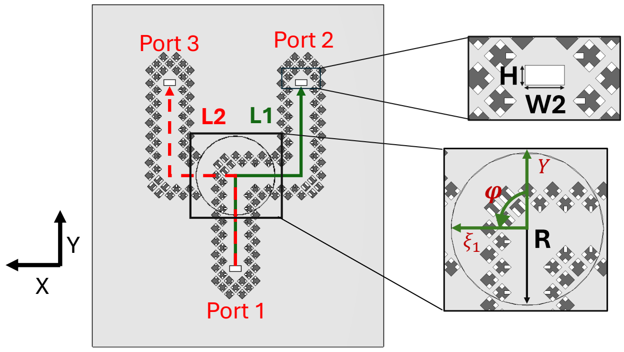

Fig. 5. Top view showing the detailed geometrical parameters. The parameter R denotes the radius of the rotating part, which is implemented in every layer.

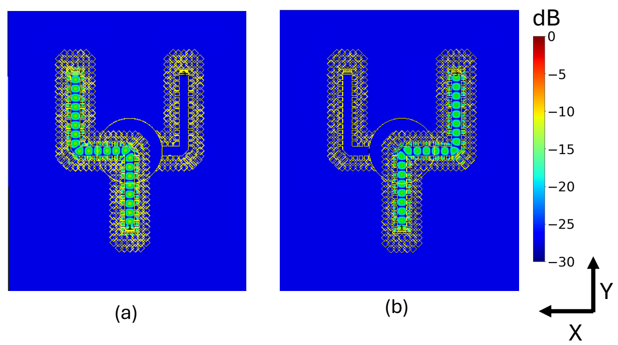

Fig. 8. Electric-field distribution at 260 GHz for different rotation angles of the moving part: (a) $\varphi = 0°$ and (b) $\varphi = 90°$.

S_{31} and $S_{11}(\varphi = 90°)$ are obtained.

The S_{21} and S_{31} parameters remain above -2 dB in the frequency range from 230 to 300 GHz, almost fully covering the H-band.

The main difference between the parameters S_{21}, $S_{11}(\varphi = 0°)$ and S_{31}, $S_{11}(\varphi = 90°)$ is attributed to the rotary part not having exactly the same shape when it is rotated. This is illustrated in Fig. 7, where it can be observed that the position of the slots is not identical when the structure is rotated to $\varphi = 90°$. The Figure shows only the layer 3. The

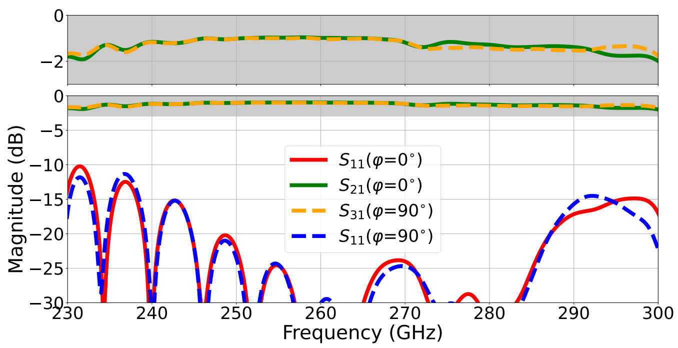

Fig. 6. S-parameters of the structure. S_{21} shows insertion losses of about 2 dB, and S_{11} a return loss better than -15 dB across most of the band.

slots cannot be placed perfectly symmetrically due to manufacturing constraints. This asymmetry is present all layers, not shown in Fig 7 for clarity. For both angles of orientation, the reflection coefficient Is below -10 dB for all frequencies under consideration, and it is below $-15dB$ in $(240 - 285$ GHz). These results confirms that the switch functions correctly in both branches.

Rotational asymmetry of the structure, This affects the S-parameter behavior.

In Fig. 8, the E-field distribution of the structure at 260 GHz is shown. The figure illustrates the E-field when the rotating part is at Fig. 8(a) and Fig. 8(b). It can be observed that the E-field remains confined within the groove along the entire propagation path.

III. Conclusion and Perspectives

In this paper, an SPDT in MLW technology has been presented by making use of a glide-symmetric unit cell as an EBG to prevent leakage in the operating band.

The designed SPDT has been demonstrated in simluations to be capable of switching between two branches, exhibiting return losses above 10 dB and insertion losses below 2 dB in both branches when rotating the switch. It is worth noting that the structure has a total thickness of only $0.5, \text{mm}$, this includes the rotating part, which makes it both lightweight and compact. This feature enables electrical actuation of the switch using a miniature motor that does not require high power.

In a future work, the implementation of the mechanical part and additional layers to integrate antennas on the structure will be carried out.

ACKNOWLEDGMENT

This publication is based on work from the Horizon EU Research and Innovation Program and UKRI under the GENIUS Project (GA: 101072560), and by the project "MedWaveImage", funded by Interreg Central Europe (CE0200670).The work is also partially funded by Sweden Vetenskaprådet project HI-CORE (2023-05184).

REFERENCES

[1] K. Rasilainen, T. D. Phan, M. Berg, A. Pärssinen, and P. J. Soh, "Hardware Aspects of Sub-THz Antennas and Reconfigurable Intelligent Surfaces for 6G Communications," *IEEE Journal on Selected Areas in Communications*, vol. 41, no. 8, pp. 2530–2546, 2023.

[2] K. Rikkinen, P. Kyosti, M. E. Leinonen, M. Berg, and A. Parssinen, "THz Radio Communication: Link Budget Analysis toward 6G," *IEEE Communications Magazine*, 2020.

[3] W. Y. Yong, A. Vosoogh, A. Bagheri, C. Van De Ven, A. Hadaddi, and A. A. Glazunov, "An Overview of Recent Development of the Gap-Waveguide Technology for mmWave and Sub-THz Applications," *IEEE Access*, vol. 11, pp. 69 378–69 400, 2023.

[4] P.-S. Kildal, E. Alfonso, A. Valero-Nogueira, and E. Rajo-Iglesias, "Local Metamaterial-Based Waveguides in Gaps Between Parallel Metal Plates," *IEEE Antennas and Wireless Propagation Letters*, vol. 8, pp. 84–87, 2009.

[5] M. Ebrahimpouri, E. Rajo-Iglesias, Z. Sipus, and O. Quevedo-Teruel, "Cost-Effective Gap Waveguide Technology Based on Glide-Symmetric Holey EBG Structures," *IEEE Transactions on Microwave Theory and Techniques*, vol. 66, no. 2, pp. 927–934, 2018.

[6] A. Vosoogh, H. Zirath, and Z. S. He, "Novel Air-Filled Waveguide Transmission Line Based on Multilayer Thin Metal Plates," *IEEE Transactions on Terahertz Science and Technology*, vol. 9, no. 3, pp. 282–290, 2019.

[7] S. Garcia-Martinez, D. Santiago, A. Tamayo-Dominguez, P. Sanchez-Olivares, I. Arregui, T. Lopetegi, M. A. G. Laso, and J. Manuel Fernandez-Gonzalez, "Robust Filter Design Built in a Contactless Metallic Multilayer Waveguide at W-Band," *IEEE Transactions on Microwave Theory and Techniques*, vol. 73, no. 9, pp. 5841–5850, 2025.

[8] O. Quevedo-Teruel, Q. Chen, F. Mesa, N. J. G. Fonseca, and G. Valerio, "On the Benefits of Glide Symmetries for Microwave Devices," *IEEE Journal of Microwaves*, vol. 1, no. 1, pp. 457–469, 2021.

[9] R.-B. Lai, J.-J. Kuo, and H. Wang, "A 60–110 GHz Transmission-Line Integrated SPDT Switch in 90 nm CMOS Technology," *IEEE Microwave and Wireless Components Letters*, vol. 20, no. 2, pp. 85–87, 2010.

.